2023 IEEE/RSJ International Conference on Intelligent Robots and Systems (IROS)
October 1-5, 2023. Detroit, USA

Soft Robot Shape Estimation: A load-agnostic geometric method

Christian Sorensen[1] and Marc D. Killpack[1]

***Abstract*— In this paper we present a novel kinematic representation of a soft continuum robot to enable full shape estimation using a purely geometric solution. The kinematic representation involves using length varying piecewise constant curvature segments to describe the deformed shape of the robot. Based on this kinematic representation, we can use overlapping length sensors to estimate the shape of continuously deformable bodies without prior knowledge of the current loading conditions. We show an implementation that assumes one change in curvature along the length of a joint, using string potentiometers as an arc length sensor, and an orientation measurement from the tip of the continuum joint. For 56 randomized joint configurations, we estimate the shape of a $250\,\mathrm{mm}$ long continually deformable robot with less then $2.5\,\mathrm{mm}$ of average error. The average error is reported for each of the 10 different equally spaced points along the length, demonstrating the ability to accurately represent the full shape of the soft robot.**

I. INTRODUCTION

Despite the potential of soft robots to interact with their environment in ways that are difficult for their rigid counterparts, soft robots may fail to realize that potential due to their inability to perceive and interpret those interactions. Without sensing methods and control algorithms that include the effects of these interactions, we expect that effective soft robot actions in uncertain environments will be limited. Load-agnostic configuration estimation (meaning that the method does not rely on accurate knowledge of loading conditions) is a difficult problem that will not likely be solved by a single estimation scheme. However, in this paper we propose an approach that enables real-time estimation of a deformable robot's shape as a first step in tackling this problem. We choose an approximation that leverages multiple connected constant curvature segments since many soft robots can be accurately described by a series of constant curvature segments (see [1], [2]). Specifically, we construct a shape estimation algorithm based on geometric properties instead of on material properties, configurations, or loading conditions. We then apply the method on a continuum soft robot as described by Allen et al. [3] (see Fig. 1). However, the method we present is general enough to work for other similar deformable robots with length sensors that span the shape of said robot. The inclusion of length sensors as described in [4] would allow this scheme to be used in fully soft robots such as those described by Williamson et al. [5].

We call the proposed geometric parametrization "length varying piecewise constant curvature" (LVPCC), and it allows for accurate representation of a continuum of complex shapes.

[1]Robotics and Dynamics Lab, Department of Mechanical Engineering, Brigham Young University, Provo, UT, USA

The continuous shape measurement capability of the sensors used in this method surpasses the limitations of discrete sensors, such as strain gauges, that only measure local curvature. The use of overlapping length sensors enables the measurement of both curvature and changes in curvature along the length of the overlap, offering the potential for efficient shape estimation with a limited number of sensors through intelligent data interpretation. The approach proposed here is also appealing because it relies solely on geometric measurements, specifically lengths and angles, rather than dynamic measurements like forces and torques, enabling shape estimation without the need for information about loading conditions. The method requires as few as three analog sensors and remarkably low computational resources, which makes it suitable for real-time proprioceptive estimation applications.

Fig. 1: Soft robotic actuator used in this paper. Length sensors are circled in blue and the camera that is used as an orientation sensor is circled in red. For this paper only the two sensors on the right of the image were used.

The contributions of this paper are:

- We derive a geometric representation of a soft robot based on piecewise constant curvature (PCC) segments whose lengths (or point of inflection) can vary. This shape estimation scheme can handle large deflections (which are representative of large external loading conditions), and uses only geometric information without knowledge of loading conditions.
- We implement a sensing-based solution of this representation that makes use of two string potentiometers and one inertial measurement unit (IMU) orientation sensor.
- We perform validation and evaluation of the above.

II. RELATED WORK

Methods and sensors for soft robot shape estimation are as diverse and varied as the different types of soft robots that have been designed and produced. We first outline the

2023 IEEE/RSJ International Conference on Intelligent Robots and Systems (IROS) | 978-1-6654-9190-7/23/$31.00 ©2023 IEEE | DOI: 10.1109/IROS55552.2023.10342225

different types of sensors used to estimate the shape of soft robots, then discuss the use of different types of models.

Some shape sensors are as simple as resistive length measurements, [6]–[9], or inductive measurements [10], [11]. Some use capacitive and pneumatic sensing combined with numerical finite element models [12]. Others remove the proprioceptive estimation problem from the robot by using cameras external to the robot to capture images which allow for 3D representation of the robot's shape [13]–[15]. Many of these methods are limited in that they provide information only at discrete locations along the length of the soft robot, which means that they can only accurately describe those points and a model has to be used to fill in the gaps (i.e. Constant Curvature, Variable Curvature, etc.). Some methods attempt to circumvent this problem by sensing and using only the end effector pose (see [16], [17]). While effective, these methods ignore the rich information that could be gained by understanding the full shape of the robot and can only be used to control the tip or end of a continuum segment, rather than the entire soft robot.

Along with these simple measurement systems there are more complicated sensing methods that rely on optical sensors such as Fiber Bragg Gratings [18]–[20]. These methods however are not easily generalized to different platforms. For example in [21] they require a camera to be able to see down the interior of the robot and use a learned model to return position based on the view of IR reflective markings on the inside of the joint. If the robot is not constructed such that a camera placed on the inside can observe along the length of the robot then the method would not work. Additionally certain changes in the arrangement of the markings led to failed estimation. Other optical fiber-based methods are combined with a simplified model to enable Kalman Filter-based estimation [22].

Machine learning in soft robotics control and estimation is very active area of research [23]–[25]. Many of these methods require platform-specific assumptions that make these models brittle. These assumptions may be eliminated as research continues, however, due to their very nature, learned models pose the risk of being uninterpretable or being used as a black box. As a direct result, the behavior of these models becomes very difficult to predict, and extrapolating outputs for conditions without training data can be dangerous.

As alternatives to machine learning, many researchers have attempted to develop analytical models to describe soft robots' shape as they deform. The most basic of these is the constant curvature (CC) model which says that the whole shape of the soft robot or continuum joint can be described by one circular arc. Because of its relative simplicity, much of the work in soft robotics is based on this model [16]. Additionally many groups take this approach and by serially connecting very short segments they create a piecewise constant curvature (PCC) robot [26]. The LVPCC model we present in this paper is based on this idea, but importantly, we add the ability of the segments to change in length. Other similar methods exist, including

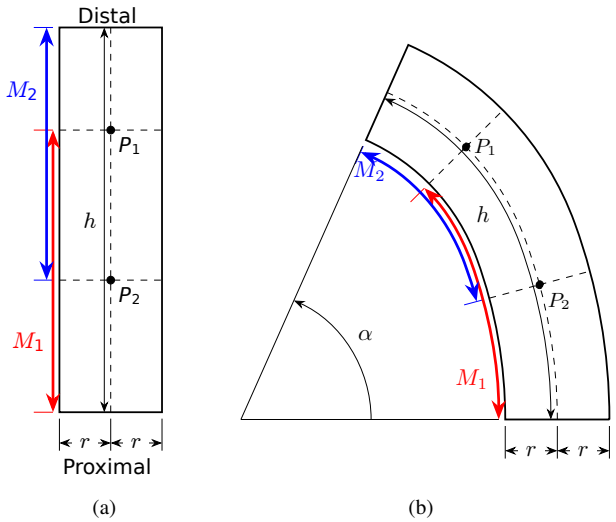

(a) (b)

Fig. 2: A planar geometric representation of a soft robot. On the left shows the robot when undeformed. M_1 and M_2 represent lengths measured at a distance r away from the center line. Points P_1 and P_2 are the point on the center line where the measurements attach. h is the center line length of the joint. The image on the right shows the same joint, but deformed. Notice that M_1 and M_2 have both decreased in magnitude, but the distance along the center line where they attach is still fixed. α represents the total change in orientation from the proximal to distal end of the robot.

the Variable Curvature method [27], polynomial fitting [28] and others [29], [30]. These methods accurately model some shapes of soft robots during operation, but rely heavily on predetermined parameters (such as sensor placement) to understand robot geometries. LVPCC removes this reliance by observing information about the majority of the robot, not just discrete points, and allowing that information to drive the estimation. It should be noted as well that dynamic models are also used to estimate the shape of soft robots, such as Cosserat Rod models [31]–[33] and Pseudo rigid body models [34], [35]. These methods remain difficult due to the need for accurate system identification. By basing our method solely on geometric relationships, it is generalizable to any geometrically similar platform.

III. Geometric Model

Fig. 2 shows a planar representation of a soft bodied joint with sensors attached, in a deformed (Fig. 2b) and undeformed (Fig. 2a) state. M_1 represents the length reported by a length sensor that attaches to the proximal end of the robot, and M_2 represents the length reported by a sensor that attaches to the distal end of the robot. P_1 and P_2 represent the point along the center line at which these sensors attach. That is to say, the distance from the proximal end of the robot to P_1 is equal to M_1 in the straight configuration, and the distance from the distal end of the robot to P_2 is equal to M_2, it should be noted that P_1 and P_2 are not necessarily the same distance away from the ends of the robot and that

$P_1, P_2 \in [0, 1]$. The surface that M_1 and M_2 are measuring is offset a distance r from the center line. h is the length of the center line. The deformed joint shown in Fig. 2b shows the same geometric representation of the robot, this time in a deformed or deflected state. M_1 and M_2 have changed length, but the distance along the center line to the points where they attach, P_1 and P_2, has not changed. The distances h and r have also been assumed to remain the same, but there is a new variable α that represents the change in orientation from the proximal to distal end of the robot. Undeformed, α is equal to zero and M_1 and M_2 are equal to $P_1 * h$ and $P_2 * h$ respectively.

The Length Varying Piecewise Constant Curvature (LVPCC) model proposed here takes the deflected state of the robot and assumes that it can be adequately represented by dividing the total deformed shape into two sequential circular arcs sharing a tangency constraint, but with an unknown inflection point. The length varying aspect indicates that each arc's length can change. An example of these two sequential circular arcs can be seen in Fig. 3. These arcs are modeled as lying along the center line of the robot, and as such the sum of these two arc lengths is equal to h. Offsetting both of these arcs by a distance of $\pm r$ results in the length of the surface measured by M_1 and M_2. The sign of the offset is determined by the location of the center of curvature of each arc. If the center of curvature is found on the same side of the arc as the measurement surface, the sign of the offset is negative, if it is found on the opposite side it is positive. In other words if the bending is towards the length sensors, the sign is negative, and away from the length sensors the sign is positive. A positive offset means the length sensor will return a measurement greater than when the joint is straight and a negative offset means the sensor will return a measurement less than when the joint is straight. The sum of the angle between the normal to the tangent of the first arc at its origin, and the normal to the tangent of the second arc at its end point is equal to α. The point at where these two arcs meet is referred to as the transition point, P_t. The location of P_t will be represented here as a fraction of the total arc length, for example if P_t is located halfway along the length of center line then $P_t = 0.5$. By modeling the joint in this way, and allowing the transition point to change, more complex shapes can be estimated then with standard piecewise constant curvature models, where the segments of constant curvature are fixed length. A representation of this model can be seen in Fig. 3 where a "c" shaped robot has been represented with a long segment of relatively small curvature followed by a short segment of relatively large curvature. Combining differing lengths of differing curvatures allows the model to accurately represent a large variety of shapes.

In order to use this model to estimate soft robot shape, the relationship between the measurements M_1, M_2, α and parameters which describe the shape need to be identified. In the interest of space only the resultant relationships are shown here, the derivation of which can be found in Chapter 3 of [36]. These equations are the following (where the quantities for A and B are intermediate variables used for convenience only):

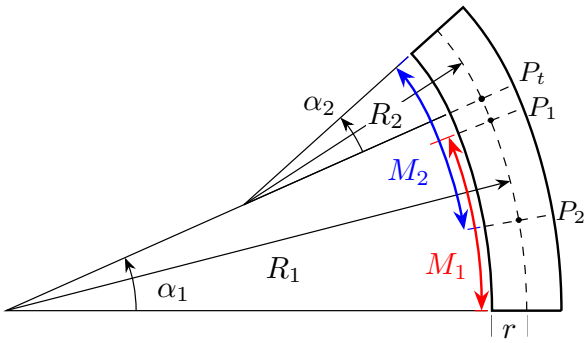

Fig. 3: A planar deformed version of a soft robot with the LVPCC model applied to it. Although in this case the change of curvature occurs in the middle of the robot, the model allows for the change to happen at any point along the length.

$$
\begin{aligned}
A_1 &= P_2\Big(M_1 - P_1 h + P_1 \alpha r\Big) \\
B_1 &= h - M_2 - P_1 h - P_2 h - \alpha r \\
&\quad + M_1 P_2 + M_2 P_1 + P_1 \alpha r + P_2 \alpha r \\
&\textbf{and} \\
P_t &= \frac{A_1}{B_1}
\end{aligned} \tag{1}
$$

$$
\begin{aligned}
A_2 &= P_1 h^2 - M_1 h + M_1 M_2 + P_1 \alpha^2 r^2 \\
&\quad + M_1 P_2 h - M_2 P_1 h + M_1 \alpha r \\
&\quad - P_1 P_2 h^2 + M_2 P_1 \alpha r \\
&\quad - 2 P_1 \alpha h r + P_1 P_2 \alpha h r \\
B_2 &= h r - M_2 r - \alpha r^2 + M_1 P_2 r + M_2 P_1 r \\
&\quad - P_1 h r - P_2 h r + P_1 \alpha r^2 + P_2 \alpha r^2 \\
&\textbf{and} \\
\alpha_1 &= \frac{A_2}{B_2}
\end{aligned} \tag{2}
$$

$$
\begin{aligned}
A_3 &= -\Big(P_1 h^2 - M_1 h + \alpha^2 r^2 + M_1 M_2 \\
&\quad - P_2 \alpha^2 r^2 + M_1 P_2 h - M_2 P_1 h + M_1 \alpha r \\
&\quad + M_2 \alpha r - \alpha h r - P_1 P_2 h^2 - M_1 P_2 r \alpha \\
&\quad - P_1 \alpha h r + P_2 \alpha h r + P_1 P_2 \alpha h r\Big) \\
B_3 &= h r - M_2 r - \alpha r^2 + M_1 P_2 r \\
&\quad + M_2 P_1 r - P_1 h r - P_2 h r \\
&\quad + P_1 \alpha r^2 + P_2 \alpha r^2 \\
&\textbf{and} \\
\alpha_2 &= \frac{A_3}{B_3}
\end{aligned} \tag{3}
$$

In these equations the configuration parameters that are used to describe the shape are α_1, α_2 and P_t. α_1 and α_2 represent the angles between the start and end of the first and second segments of curvature respectively, and P_t is a fraction representing the location along the center line of the start of the second segment of constant curvature. Using these equations and the three proposed measurements, the soft robot shape can be modeled.

IV. Hardware

In order to validate the developed model, real-world tests were performed on a soft continuum robot joint. The hardware platform that was used for this purpose is a pneumatic hybrid rigid-soft robot joint shown in Fig. 1. This platform and serially connected versions have been studied in [1], [3], [16]. It consists of 4 blow-molded bellows located around an inextensible cable acting as a spine. For the purposes of validating this estimation model and method we manually applied a force and moment to deflect the robot and cause non-constant curvature across the entire joint. Part of this test was to see how well two constant curvature segments could approximate the actual joint shape. The sensors that we used consist of two spring potentiometers made by Unimeasure [37]. These are rotary potentiometers where the resistance seen across two legs of the potentiometer is linearly related to the amount that the potentiometer has turned. They have a constant spring return force of $2.2\,\mathrm{N}$ and an output of approximately $10\,\mathrm{mV/mm}$ with $5\,\mathrm{V}$ excitation. An Arduino Mega with a breakout I2C Analog to Digital Converter board was used to read in the output voltage of the potentiometers and convert the voltage into lengths. This data is then sent over the Arduino's serial line via a USB cable to a host computer which combines these length measurements and an orientation measurement of the tip of the joint to estimate the shape of the robot. In order to measure the change in orientation from the base of the joint to the end, the IMU data from a ZED Mini is used. The ZED Mini outputs a filtered version of the IMU data, which is available at $100\,\mathrm{Hz}$. It should be noted that the ZED camera's IMU was used because it was available, but that any device that measures relative orientation could be used instead (including the visual odometry provided by the ZED Mini if used in a feature-rich environment).

V. Experiments

To evaluate the performance of the model and sensing method, we compared the center line of our soft robot as estimated by our algorithm with the actual center line position. To measure the ground truth of the center line position we attached a set of IR reflective Cortex Motion Capture dots to our hardware platform. We then inflated the robot to a pressure, and manually deflected it via a winch-driven cable attached to the top of the joint (see Fig. 4). After deflection, we measured the location of these IR dots. To ensure the deflection was planar for these experiments, the robot was made to deform along a rigid backstop which can be seen in Fig. 4. In addition to the LVPCC

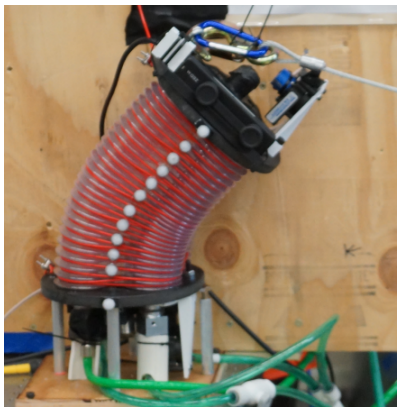

Fig. 4: A picture of the 2D experimental setup. The back plate that was used to constrain the deformation of the joint to a plane is the wood panel seen here. In white are the Motion capture dots that were observed as ground truth.

estimation, we recorded the deflected angle of the end of the joint and estimated a single constant curvature shape for comparison as done in [3], [16], [17]. It should be noted that the comparison to constant curvature is not done because constant curvature estimation is expected to be accurate for the deflections seen here, but because it provides a simple and effective benchmark to compare estimation methods. Any comparison with other PCC methods would require us to assume the location of the piecewise constant curvature sections. However, this is exactly the strength of the approach in this paper (that we estimate an inflection point as part of the process). In addition, comparison to a constant curvature model shows that the configurations we chose were indeed poorly described by a single circular arc and are therefore good configurations for evaluating our algorithm.

We repeated this test for 56 different joint configurations. For each of the configurations measured, two seconds of data was collected, and the estimated values were averaged across that time, with a sensor update rate of $\approx 100\,\mathrm{Hz}$. Fig. 5 shows a simplified representation of six of these configurations, and a video showing all 56 configurations can be seen here: `https://youtu.be/WfbcGrP8cpo`. It is important to remember that the motion capture data is *only* used for ground truth comparison, not for shape estimation.

VI. Results

The results in Fig. 5 show the qualitative performance of this algorithm. In terms of quantitative results, we start by examining the distribution of error for all markers at each configuration. Fig. 6 shows box plots representing the distance from each IR marker to the predicted center line for a random sampling of 28 of the configurations tested. The black box represents the 25th and 75th percentiles and the cyan line represents the median value, with whiskers representing values lying within 1.5 of the inter-quartile range from the median. Each box represents the distribution of the errors for all markers averaged over a two second window. For example, for configuration 19 using the LVPCC

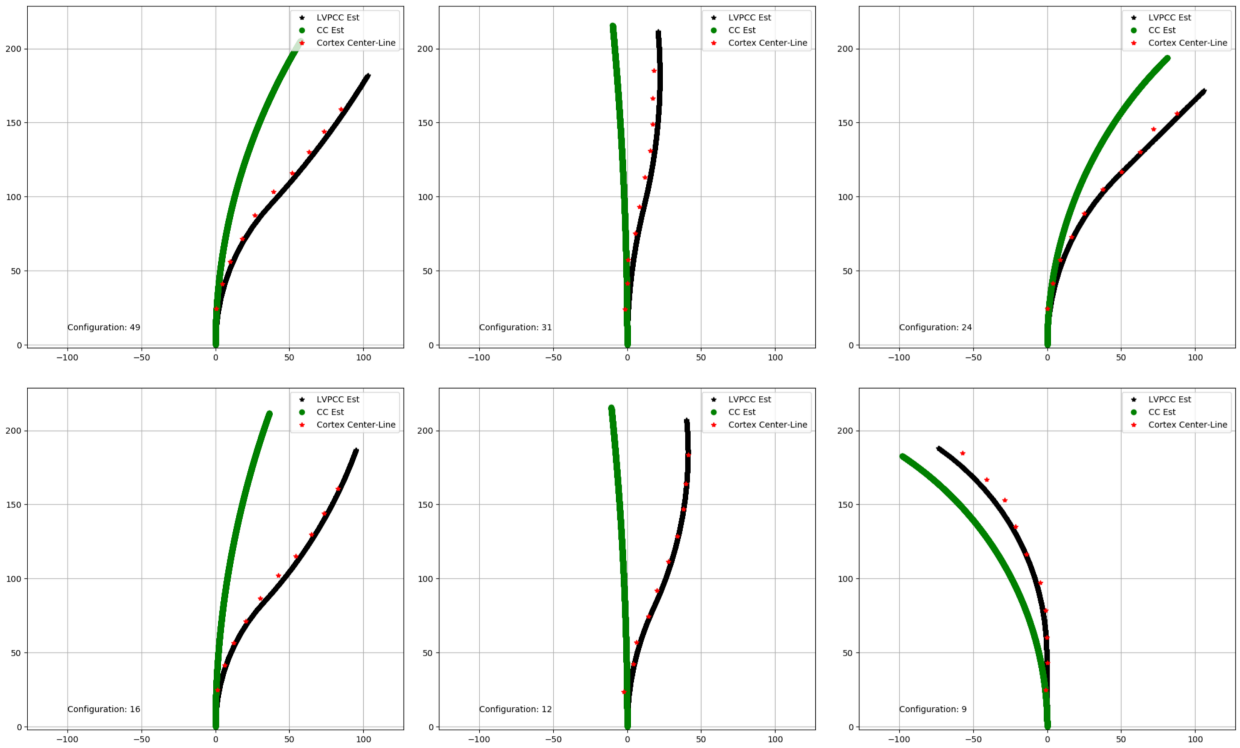

Fig. 5: Six representative configurations realized during the course of the experiment. The green line represents a constant curvature model fit. The black represents the proposed LVPCC model, and the red represents ground truth data taken by the Cortex Motion capture system.

model, the highest error was less then $10\,\mathrm{mm}$ (seen in the figure as an outlier) and the lowest was below $2\,\mathrm{mm}$. This is of course assuming that the motion capture measurements for ground truth are perfectly accurate, and that the IR markers do not shift relative to the soft deformable robot (neither of which is completely true).

Both methods, constant curvature (CC) and the length varying piecewise constant curvature (LVPCC), were compared. Across all of the 56 configurations the average median error (found by averaging the median error of all 56 configurations) was $16.61\,\mathrm{mm}$ for the CC and the average median error was $2.35\,\mathrm{mm}$ for the LVPCC method, or in other words the error was approximately seven times larger for the CC method as opposed to the LVPCC. The minimum median error (calculated as the minimum of the list of median errors) across all 56 configurations was $2.13\,\mathrm{mm}$ for the CC method and only $0.79\,\mathrm{mm}$ for the LVPCC method.

Another interesting way of looking at the data from the experiment is looking at the error at each marker across the different joint configurations. Fig. 7 shows the average error across all 56 configurations reported as a single number for each marker, with "0" being the marker closest to the proximal end and "9" being the marker closest to the distal end. For the LVPCC method the average error does not significantly increase for the markers from proximal ($2.43\,\mathrm{mm}$) to distal ($2.6\,\mathrm{mm}$). For the CC method the error significantly increases from the proximal ($1.05\,\mathrm{mm}$) to distal ($33.69\,\mathrm{mm}$) markers. It makes intuitive sense that the proximal end of the joint has low error for both methods, because it is so close to the origin, it would require significant curvature for the error to be large. However the fact that the average error per marker does not grow as the distance from the origin to the marker under consideration increases seems to indicate that the shape is well estimated by the LVPCC method, and that the shape is unsurprisingly not well estimated by the CC method.

Finally in Fig. 8 we show the distribution of the error for all markers and all configurations for each of the two estimation methods. This is in contrast to the summary statistics that we first presented. Overall, the LVPCC method results in a much tighter distribution with a much lower mean or median error. While the CC method has higher error and variance. The mean and median errors are $2.55\,\mathrm{mm}$ and $2.28\,\mathrm{mm}$ for LVPCC, and $17.05\,\mathrm{mm}$ and $12.81\,\mathrm{mm}$ for CC respectively. This shows that for a wide range of non-trivial loading conditions, the LVPCC method presented provides better accuracy and precision.

VII. Future Work and Conclusion

The work presented in this paper is the first stage of developing LVPCC model. By validating this model in two dimensions, we prove its merit which shows the value of further research into the important extension to three dimensions. This extension is ongoing, but holds promise, with all the same advantages presented in Section I applying to the

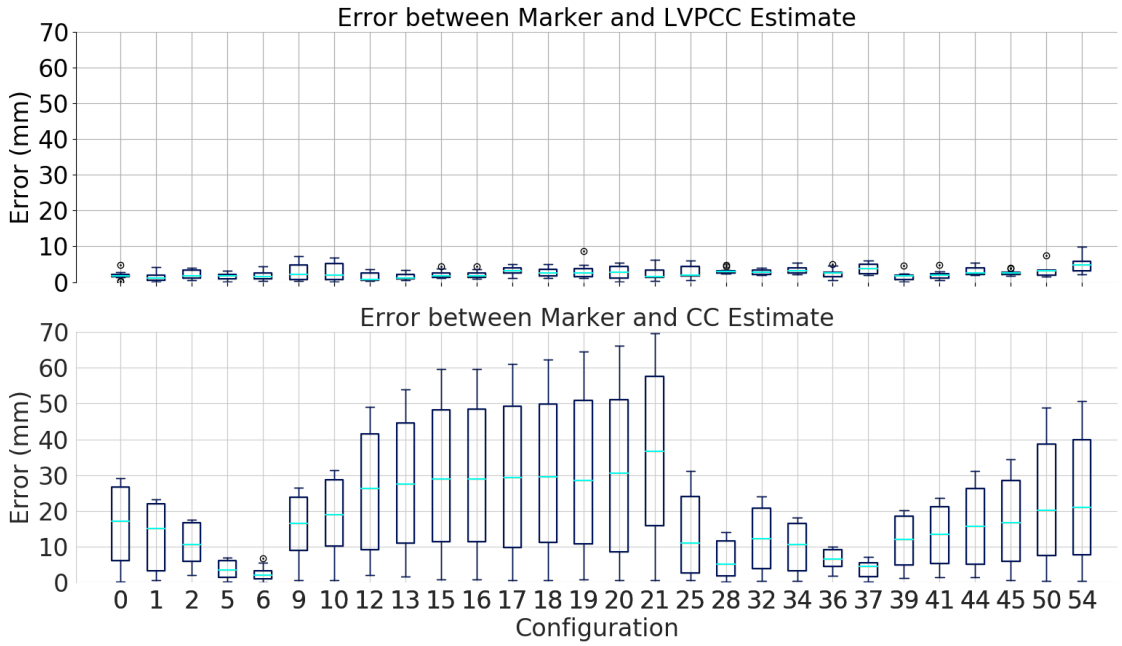

Fig. 6: Box plots showing the distribution of error for 28 of the 56 configurations. For some of the configurations the CC model approximated the error quite well (e.g. 6 and 37) however for the majority of configurations the LVPCC model significantly outperformed the CC model in terms of estimating the robot's shape.

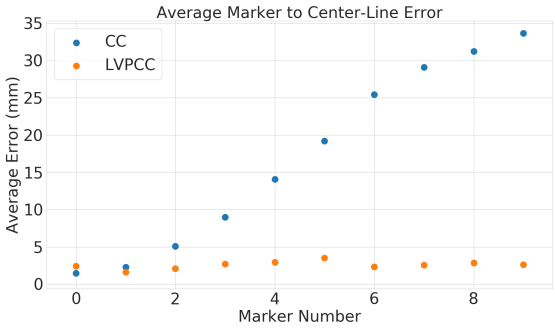

Fig. 7: Scatter plot showing average error associated with each marker. The numbers 0 through 9 represent markers placed proximally to distally.

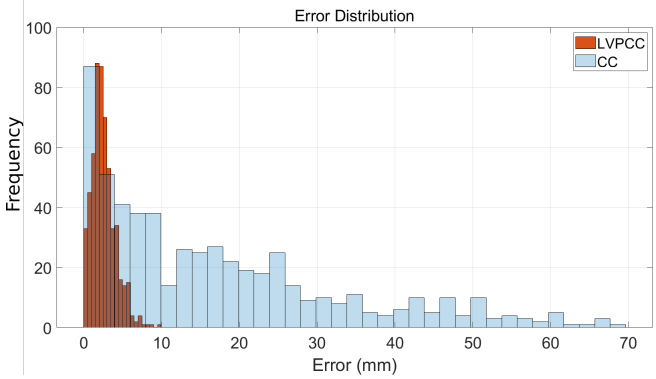

Fig. 8: Histogram showing the distribution of the errors for all markers across all configurations. The LVPCC method has a much smaller spread as well as having a lower average error. The CC method's spread is large, and its average error is close to 7 times the average error of the LVPCC method.

three dimensional case. Preliminary results are encouraging but have raised several difficulties (e.g. measurement of singularities in the 3D case, the effect of torsion about the central axis), that need to be addressed. In order to extend this model to three dimensions, one more measurement of the angular deflection at the distal point of the soft robot is required. In CAD, we have already validated that by using geometric relationships the measurement can be transformed to appropriately represent the deformed length of the robot. More information on preliminary results can be seen in [36].

We have shown a novel geometric representation for a continuum soft robot joint consisting of three configuration variables that can be analytically determined with the use of three simple measurements. Due to the geometric nature of this model, it is applicable to any similarly shaped robot or any robot that could be accurately represented in such a way. This includes more compliant soft robots where multiple segments can represented with LVPCC by combining multiple length measurements at fixed intervals serially to approximate and estimate the true shape (similar to what was done in simulation in [38]). We have implemented this model on a real soft robot and showed that it accurately represents the shape of the robot, with less then $2.5\,\mathrm{mm}$ of median

error for a joint that is $250\,\mathrm{mm}$ long. Additional work needs to be done to validate estimation for 3D deformation, and to evaluate the feasibility of this method for use in a real-time control algorithm, although both the electronics for data acquisition, and the algorithm complexity are simple enough that this should not be a concern. Finally the algorithm will need to be evaluated for singularities, and modifications to improve robustness near the singularities may be needed to estimate shape consistently across the whole workspace.

ACKNOWLEDGEMENTS

This work was supported by the National Science Foundation under Grant no. 1935312.

REFERENCES

[1] L. Rupert, T. Duggan, and M. D. Killpack, "Improved continuum joint configuration estimation using a linear combination of length measurements and optimization of sensor placement," *Frontiers in Robotics and AI*, vol. 8, 2021.

[2] R. K. Katzschmann, C. Della Santina, Y. Toshimitsu, A. Bicchi, and D. Rus, "Dynamic motion control of multi-segment soft robots using piecewise constant curvature matched with an augmented rigid body model," in *2019 2nd IEEE International Conference on Soft Robotics (RoboSoft)*. IEEE, 2019, pp. 454–461.

[3] T. F. Allen, L. Rupert, T. R. Duggan, G. Hein, and K. Albert, "Closed-form non-singular constant-curvature continuum manipulator kinematics," in *2020 3rd IEEE International Conference on Soft Robotics (RoboSoft)*, 2020, pp. 410–416.

[4] B. Oldfrey, R. Jackson, P. Smitham, and M. Miodownik, "A deep learning approach to non-linearity in wearable stretch sensors," *Frontiers in Robotics and AI*, vol. 6, 2019.

[5] J. G. Williamson, C. Schell, M. Keller, and J. Schultz, "Extending the reach of single-chamber inflatable soft robots using magnetorheological fluids," in *2021 IEEE 4th International Conference on Soft Robotics (RoboSoft)*, 2021, pp. 119–125.

[6] P. T. Gibbs and H. H. Asada, "Wearable Conductive Fiber Sensors for Multi-Axis Human Joint Angle Measurements," *Journal of NeuroEngineering and Rehabilitation*, vol. 2, no. 1, p. 7, 2005.

[7] K. Elgeneidy, N. Lohse, and M. Jackson, "Data-Driven Bending Angle Prediction of Soft Pneumatic Actuators with Embedded Flex Sensors," *IFAC-PapersOnLine*, vol. 49, no. 21, pp. 513–520, 2016.

[8] M. C. Yuen, H. Tonoyan, E. L. White, M. Telleria, and R. K. Kramer, "Fabric sensory sleeves for soft robot state estimation," in *Robotics and Automation (ICRA), 2017 IEEE International Conference on*. IEEE, 2017, pp. 5511–5518.

[9] Y. Yang, H. Zhu, J. Liu, H. Lu, Y. Ren, and M. Y. Wang, "A proprioceptive soft robot module based on supercoiled polymer artificial muscle strings," *Polymers*, vol. 14, no. 11, p. 2265, 2022.

[10] W. Felt, M. Suen, and C. D. Remy, "Sensing the motion of bellows through changes in mutual inductance," in *2016 IEEE/RSJ International Conference on Intelligent Robots and Systems (IROS)*. IEEE, oct 2016, pp. 5252–5257. [Online]. Available: http://ieeexplore.ieee.org/document/7759772/

[11] W. Felt *et al.*, "An inductance-based sensing system for bellows-driven continuum joints in soft robots," *Autonomous robots*, vol. 43, no. 2, pp. 435–448, 2019.

[12] S. E. Navarro *et al.*, "A model-based sensor fusion approach for force and shape estimation in soft robotics," *IEEE Robotics and Automation Letters*, vol. 5, no. 4, pp. 5621–5628, 2020.

[13] M. W. Hannan and I. Walker, "Real-time shape estimation for continuum robots using vision," *Robotica*, vol. 23, no. 5, p. 645–651, 2005.

[14] E. J. Lobaton, J. Fu, L. G. Torres, and R. Alterovitz, "Continuous shape estimation of continuum robots using x-ray images," in *2013 IEEE International Conference on Robotics and Automation*, 2013, pp. 725–732.

[15] A. D. Marchese, R. Tedrake, and D. Rus, "Dynamics and trajectory optimization for a soft spatial fluidic elastomer manipulator," *The International Journal of Robotics Research*, vol. 35, no. 8, pp. 1000–1019, 2016.

[16] C. C. Johnson, T. Quackenbush, T. Sorensen, D. Wingate, and M. D. Killpack, "Using first principles for deep learning and model-based control of soft robots," *Frontiers in Robotics and AI*, vol. 8, 2021.

[17] P. Hyatt, C. C. Johnson, and M. D. Killpack, "Model reference predictive adaptive control for large-scale soft robots," *Frontiers in Robotics and AI*, vol. 7, 2020.

[18] R. Xu, A. Yurkewich, and R. V. Patel, "Curvature, torsion, and force sensing in continuum robots using helically wrapped FBG sensors," *IEEE Robotics and Automation Letters*, vol. 1, no. 2, pp. 1052–1059, jul 2016.

[19] S. Sefati, M. Pozin, F. Alambeigi, I. Iordachita, R. H. Taylor, and M. Armand, "A highly sensitive fiber bragg grating shape sensor for continuum manipulators with large deflections," in *2017 IEEE SENSORS*, 2017, pp. 1–3.

[20] S. Sefati, C. Gao, I. Iordachita, R. H. Taylor, and M. Armand, "Data-driven shape sensing of a surgical continuum manipulator using an uncalibrated fiber bragg grating sensor," *IEEE Sensors Journal*, vol. 21, no. 3, pp. 3066–3076, 2021.

[21] J. Oliveira, A. Ferreira, and J. C. Reis, "Design and experiments on an inflatable link robot with a built-in vision sensor," *Mechatronics*, vol. 65, p. 102305, 2020.

[22] D. Lunni, G. Giordano, E. Sinibaldi, M. Cianchetti, and B. Mazzolai, "Shape estimation based on kalman filtering: Towards fully soft proprioception," in *2018 IEEE International Conference on Soft Robotics (RoboSoft)*. IEEE, 2018, pp. 541–546.

[23] D. Kim *et al.*, "Review of machine learning methods in soft robotics," *PLoS One*, vol. 16, no. 2, 2021.

[24] T. G. Thuruthel, B. Shih, C. Laschi, and M. T. Tolley, "Soft robot perception using embedded soft sensors and recurrent neural networks," *Science Robotics*, vol. 4, no. 26, p. eaav1488, 2019.

[25] J. Hughes, F. Stella, C. D. Santina, and D. Rus, "Sensing soft robot shape using imus: An experimental investigation," in *Experimental Robotics*, B. Siciliano, C. Laschi, and O. Khatib, Eds. Cham: Springer International Publishing, 2021, pp. 543–552.

[26] C. Della Santina, R. K. Katzschmann, A. Biechi, and D. Rus, "Dynamic control of soft robots interacting with the environment," in *2018 IEEE International Conference on Soft Robotics (RoboSoft)*, 2018, pp. 46–53.

[27] D. Lunni, M. Cianchetti, E. Falotico, C. Laschi, and B. Mazzolai, "A closed loop shape control for bio-inspired soft arms," 07 2017, pp. 567–573.

[28] C. D. Santina and D. Rus, "Control oriented modeling of soft robots: The polynomial curvature case," *IEEE Robotics and Automation Letters*, vol. 5, no. 2, pp. 290–298, 2020.

[29] A. H. Chang, C. Freeman, A. N. Mahendran, V. Vikas, and P. A. Vela, "Shape-centric modeling for soft robot inchworm locomotion," in *2021 IEEE/RSJ International Conference on Intelligent Robots and Systems (IROS)*, 2021, pp. 645–652.

[30] J. So *et al.*, "Shape estimation of soft manipulator using stretchable sensor," *Cyborg and Bionic Systems*, vol. 2021, 2021.

[31] C. Armanini, I. Hussain, M. Z. Iqbal, D. Gan, D. Prattichizzo, and F. Renda, "Discrete cosserat approach for closed-chain soft robots: Application to the fin-ray finger," *IEEE Transactions on Robotics*, vol. 37, no. 6, pp. 2083–2098, 2021.

[32] J. Till, V. Aloi, and C. Rucker, "Real-time dynamics of soft and continuum robots based on cosserat rod models," *The International Journal of Robotics Research*, vol. 38, no. 6, pp. 723–746, 2019.

[33] F. Boyer, V. Leidiot, F. Candelier, and F. Renda, "Dynamics of continuum and soft robots: A strain parameterization based approach," *IEEE Transactions on Robotics*, vol. 37, no. 3, pp. 847–863, 2021.

[34] S. Satheeshbabu and G. Krishnan, "Designing systems of fiber reinforced pneumatic actuators using a pseudo-rigid body model," in *2017 IEEE/RSJ International Conference on Intelligent Robots and Systems (IROS)*, 2017, pp. 1201–1206.

[35] V. K. Venkiteswaran, J. Sikorski, and S. Misra, "Shape and contact force estimation of continuum manipulators using pseudo rigid body models," *Mechanism and Machine Theory*, vol. 139, pp. 34–45, 2019.

[36] C. P. Sorensen, "Soft robot configuration estimation: Towards load-agnostic soft-bodied proprioception," 2023.

[37] "Linear variable displacement transducer: Lvdt sensor," Dec 2021. [Online]. Available: https://unimeasure.com/products/lx-series/

[38] L. Rupert, T. Duggan, and M. D. Killpack, "Improved Continuum Joint Configuration Estimation Using a Linear Combination of Length Measurements and Optimization of Sensor Placement," *Frontiers in Robotics and AI*, vol. 8, 2021.